59th ILMENAU SCIENTIFIC COLLOQUIUM
Technische Universität Ilmenau, 11 — 15 September 2017
URN: urn:nbn:de:gbv:ilm1-2017iwk-049:9

OBJECT CONTOUR SENSING USING ARTIFICIAL ROTATABLE VIBRISSAE

Lukas Merker / Christoph Will / Joachim Steigenberger / Carsten Behn

Technical Mechanics Group, Department of Mechanical Engineering
Technische Universität Ilmenau
Max-Planck-Ring 12, 98693 Ilmenau, Germany
{lukas.merker, carsten.behn}@tu-ilmenau.de

ABSTRACT

Recent research topics in bionics focus on the analysis and synthesis of mammal's perception of their environment by means of their vibrissae. Using these complex tactile sense organs, rats and mice, for example, are capable of detecting the distance to an object, its contour and its surface texture. In this paper, we focus on developing and investigating a biologically inspired mechanical model for object scanning and contour reconstruction. A vibrissa – used for the transmission of a stimulus – is frequently modeled as a cylindrically shaped Euler-Bernoulli-bending rod, which is one-sided clamped and swept along an object translationally. Due to the biological paradigm, the scanning process within the present paper is adapted for a rotational movement of the vibrissa. Firstly, we consider a single quasi-static sweep of the vibrissa along a strictly convex profile using nonlinear Euler-Bernoulli theory. The investigation leads to a general boundary-value problem with some unknown parameters, which have to be determined in using shooting methods. Then, it is possible to calculate the support reactions of the system. These support reactions together with the boundary conditions to the support, which all form quantities an animal solely relies on in nature, are used for the reconstruction of the object contour. Afterwards, the scanning process is extended by rotating the vibrissa in opposite direction in order to enlarge the reconstructable area of the profile.

Index Terms— tactile sensor, bio-inspired sensor, animal vibrissa, object contour detection, rotatable movement.

1. INTRODUCTION

Tactile sensors play a key role in many engineering sectors, such as mobile robotics, production technology or quality control. These sensors are capable of characterizing objects based on mechanical contacts. The scope of common tactile sensors ranges from simple passive impact sensors to complex, integrated systems. A major benefit of tactile sensors is their suitability in environments with poor visibility, where optical sensors reach their limits. Within the present work, we focus on developing and investigating a model for object shape recognition using tactile information. Since technical solutions for this task are often inspired by nature, we give a brief overview of the biological paradigm.

Many rodents (e.g. mice and rats) use their mystacial macrovibrissae (prominent tactile hairs in their snout region) for non-visual exploration of their environment (see Fig. 1(a) and (b)).

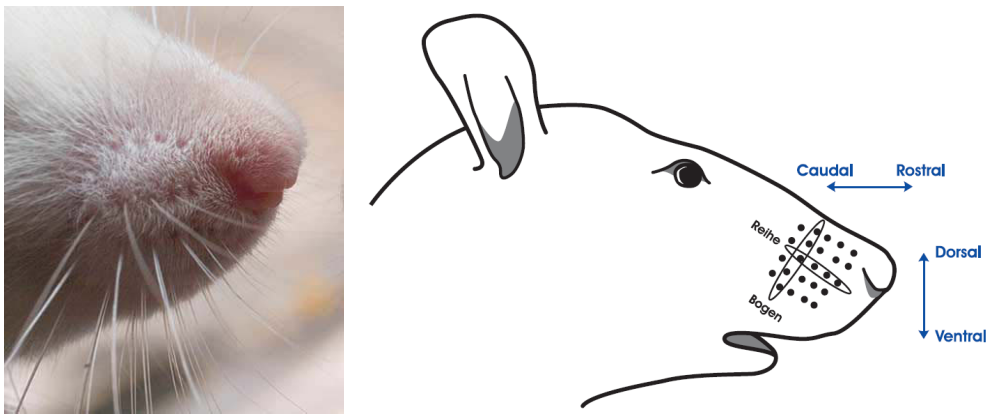

(a) (b)

Figure 1. Mystacial pad with vibrissae: (a) snout of a rat [25]; (b) schematic arrangement [3].

Vibrissae do not consist of any sensory components, but are used for the transmission of a stimulus. Thus, the perception of a stimulus does not happen in the vibrissa but in its support, the so-called follicle-sinus complex (FSC) [6], [7]. Every vibrissa is embedded in its own FSC, which consists of several mechanoreceptors converting tactile information into neural impulses for the central nervous system [6], [3], [16]. Figure 2 shows two adjacent hair follicles, which are surrounded by the extrinsic and intrinsic musculature.

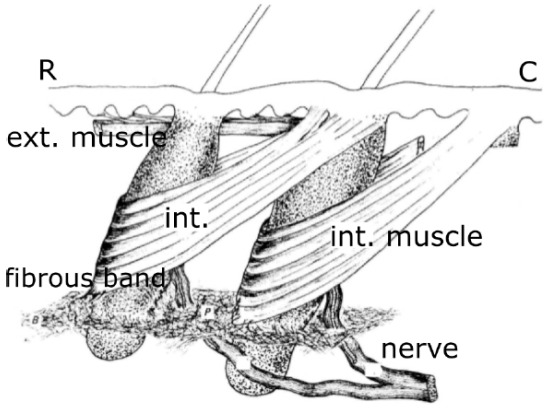

Figure 2. Schematic drawing of two adjacent hair follicles [5].

This musculature enables the animal to use its vibrissae in two different operating modes – an active and a passive one [13]:

- In passive mode, a vibrissa is deformed only by external forces (e.g. wind or mechanical contacts, when the animal passes an object) without activating the musculature. If the external force disappears, the vibrissa returns passively to its initial state due to the elasticity of the surrounding tissue or actively by activation of the extrinsic musculature [3].
- In the active exploration mode, vibrissae can be swept along an object rotationally by alternating contraction of the intrinsic and extrinsic musculature in order to detect surface or shape information of an object. This behavior, in which the vibrissae are moved back and forth repeatedly, is called “whisking”. Mice and rats are capable of controlling this movement (e.g. the frequency and amplitude) [13].

In this work, we focus on a kind of an active behavior of the vibrissa movement: Setting up a model for tactile shape recognition we limit ourselves to the main characteristics of the biological paradigm, which are given by the rotational movement of the vibrissae and the fact, that stimuli can only be detected by mechanoreceptors in the FSC. Since there are already different modeling approaches in literature, we give a short overview of the current state of the art at first.

2. STATE OF ART

In literature, biological inspired tactile sensors are used with different purposes. In the simplest case, artificial vibrissae function as binary contact detectors [9], [10] to provide information about whether there is contact with an object or not. Simple arrangements like these can be used for early identification of obstacles and collision avoidance for mobile robots. Other sensors provide more detailed information like the distance to an object, its shape or surface texture.

A vibrissa is frequently modeled as a long slim Euler-Bernoulli bending rod. The scanning process is operated by sweeping the rod along an object translationally or rotationally, that leads to a linear-elastic (assumed) deformation of the rod. Measuring different information at the support (e.g. the rod angle or the reaction forces and moment), these quantities can be used to reconstruct the object contour. Depending on the permitted deflection the deformation of the rod can be described using linear [2], [11], [19] or nonlinear [18], [4], [20], [21], [22], [23], [24], [8], [14] Euler-Bernoulli theory.

In [11], artificial whiskers were used to determine the distance to an object using the linear theory of elasticity. The model used is shown in Fig. 3.

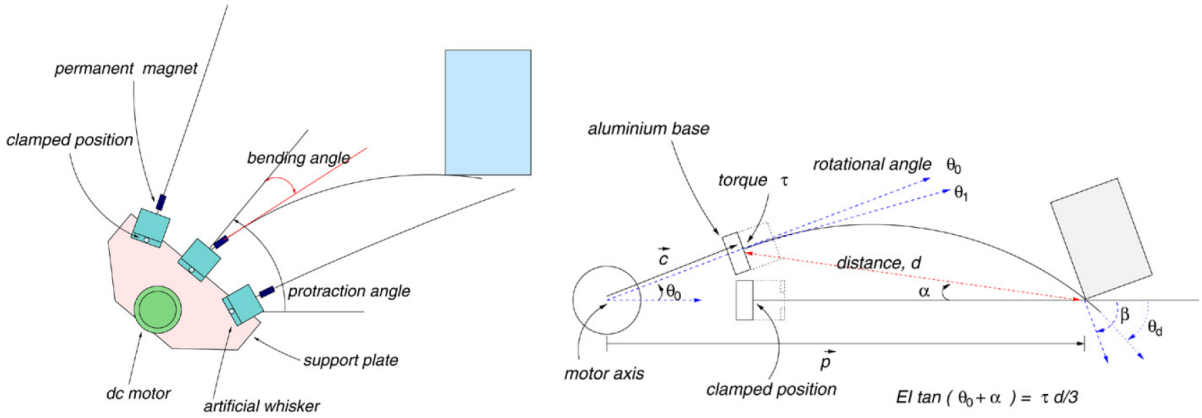

Figure 3. Model used in [11] for distance estimation.

In this case only information about the deflection angle at the support but no reaction forces or moments are required. The object distance is determined taking advantage of the angular relationships, but using the simple linear bending theory.

Since linear theory is **not** suitable for describing large deflections of a vibrissa (that actually occurs in reality), other models make use of the nonlinear Euler-Bernoulli theory. In [18], a single artificial vibrissa was swept along an object by a DC-motor as shown in Fig. 4(a). During the rotational scanning process the support reactions were measured by a load cell. The shape of the vibrissa was determined by numerically integrating the deformation equations at different points in time. Frequently repeating this procedure results in a variety of deformation states, see Fig. 4(b), that can be used for an approximation of the object contour.

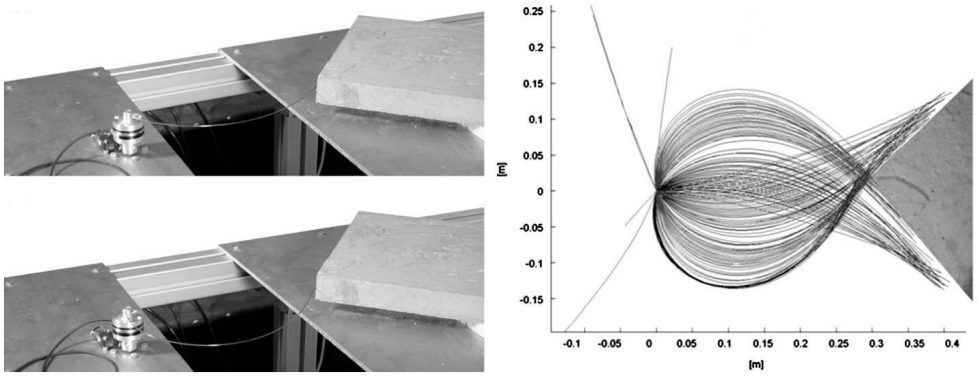

(a) (b)

Figure 4. Rotational scanning procedure in [18]: (a) prototype; (b) numerically integrated deformed states.

In [4], this approach was adapted for spatial problems.
The authors of [20], [22], [23], [24] consider a quasi-static translational sweep of an Euler-Bernoulli bending rod, which is one-sided clamped, along a strictly convex profile function. In a first step, the scanning process is treated analytically as far as possible to determine the unknown parameters (e.g. the contact force) which have to be used to calculate the support reactions. In a next step, a sequence of contact points (approximating the object contour) is determined using only the these support reactions.

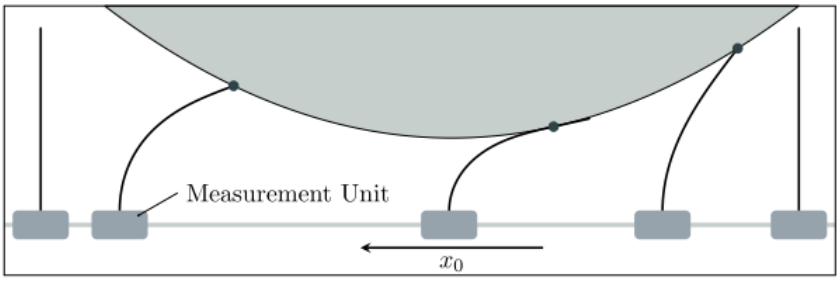

Figure 5. Translatorally scanning of a strictly convex profile function [24].

In [24], the elasticity of the support (clamping) was increased by a rotational spring in order to take the elastic properties of the FSC into account. In addition, other models consider the geometric properties of a vibrissa, especially its tapered shape and intrinsic curvature [8], [14]. In both publications, the tapering is described linear and the pre-curvature is approximated using finite differences. The authors in [1] used a polynomial of order 10 to describe the precurvature of the artificial vibrissa, that is used for object shape recognition.
Within the present paper, we will not focus on the geometrical characteristics of the vibrissae, but on the main characteristic of the rotational movement of the vibrissa. The governed results will extend and complement the ones from [22], [23], [24], [20], [21].

3. GOAL

Current models frequently describe a translationally movement of technical vibrissae. However, this does not match the behavior observed in rats and mice during active whisking. Thus, within the present paper, we focus on the following aspects:

- setting up a model of a single technical vibrissa for **rotational** object scanning and contour reconstruction;
- formulating the model equations using nonlinear Euler-Bernoulli theory for large deflections;
- describing the procedure of locating a sequence of contact points between the rod and the object (contour reconstruction), only using information at the support of the (technical vibrissa); and
- numerical simulations of the scanning process:

1. we determine the unknown support reactions and the setting moment during a single sweep,
2. we use these quantities to determine a sequence of contact points in order to approximate the object contour, and
3. afterwards, the scanning process is extended by rotating the vibrissa in opposite direction in order to enlarge the reconstructable area of the object.

4. MODELING

For the scanning process we consider a single vibrissa that is swept along an object rotationally in a mathematical positive sense, as shown in Fig. 6.

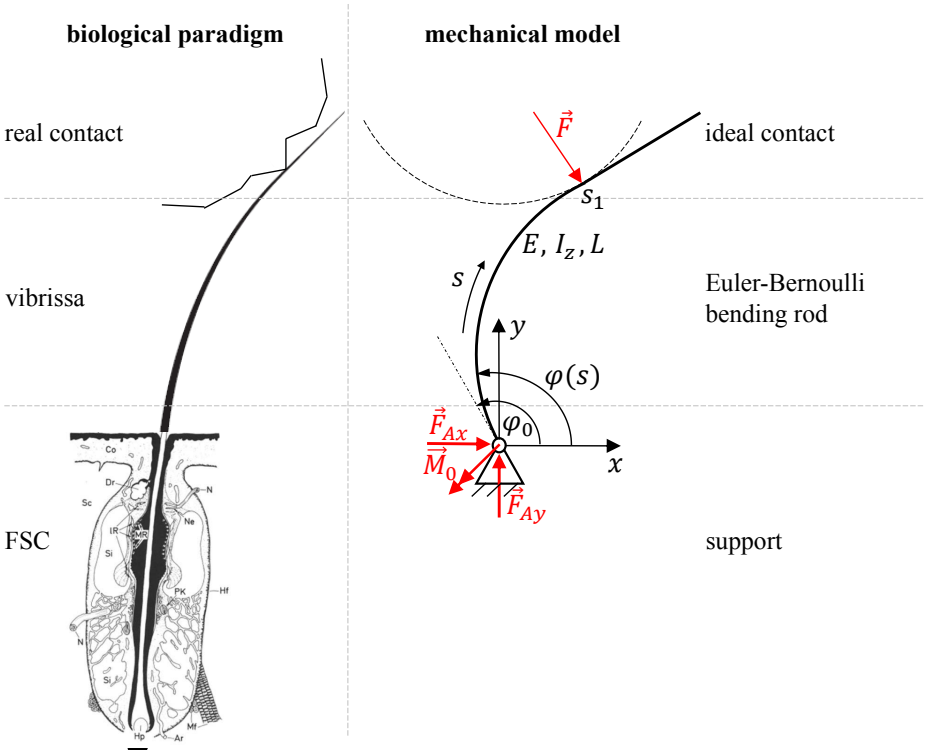

Figure 6. Modeling approach: left – schematic representation of the biological paradigm (modified from [17]); right – mechanical model in [12].

The mechanical model is based on the following **assumptions**:

- The scanning process takes place in the x-y-plane. The vibrissa rotates around the z-axis by increasing the setting angle φ_0 incrementally. Therefore, the required setting moment M_0 will be calculated.
- The rotational movement of the vibrissa is sufficiently slow, which allows to treat the scanning process quasi-statically.
- The vibrissa is modeled as a thin Euler-Bernoulli bending rod of length L, which is straight and cylindrically shaped. Its second moment of area I_z and its Young's modulus E are constant. The large deflections occurring during the scanning process are described using the nonlinear Euler-Bernoulli theory.
- The bending rod is pivoted rotationally by a bearing.
- The object is modeled as a rigid body, whose contour is considered as a strictly convex function $g : x \mapsto g(x)$. This assumption ensures that there is only one contact point between the rod and the object. Ignoring friction effects, the contact is modeled as an ideal contact. Thus, the contact force is always perpendicular to the profile tangent.

The curvature $\kappa(s)$ of the deflected beam can be described using nonlinear Euler-Bernoulli theory, as follows:

$$\kappa(s) = \frac{M_{bz}(s)}{EI_z(s)} \tag{1}$$

with bending moment $M_{bz}(s)$, Young's modulus E and second moment of area I_z, that is assumed to be constant, see above. The bending rod axis can be parameterized by means of its slope angle $\varphi(s)$ in dependence on the natural coordinate arc length s:

$$\frac{dx(s)}{ds} = \cos(\varphi(s)) \tag{2}$$

$$\frac{dy(s)}{ds} = \sin(\varphi(s)) \tag{3}$$

$$\frac{d\varphi(s)}{ds} = \kappa(s) \tag{4}$$

Remark 4.1. *To allow any kind of scaling, we introduce dimensionless variables. Therefore, all lengths are measured in L (e.g. $s := \frac{\tilde{s}}{L}, s \in [0,1]$), moments in EI_zL^{-1} and forces in EI_zL^{-2}.*

These dimensionless quantities are used to rewrite (1), (2), (3) and (4), which form a set of ordinary differential equation (ODE), describing the deflected bending rod:

$$\left.\begin{aligned} x'(s) &= \cos(\varphi(s)) \\ y'(s) &= \sin(\varphi(s)) \\ \varphi'(s) &= \kappa(s), \quad \kappa(s) = m_{bz}(s) \end{aligned}\right\} \tag{5}$$

Due to the strict convexity, the contour function $g : x \mapsto g(x)$ is parameterized by means of its slope angle $\alpha \in (-\frac{\pi}{2}, \frac{\pi}{2})$ as follows:

$$\frac{dg(x)}{dx} = \tan(\alpha)$$

$$\Rightarrow \xi(\alpha) = g'^{-1}(\tan(\alpha))$$

$$\Rightarrow \eta(\alpha) = g(\xi(\alpha))$$

Hence, each point of the contour function can be given by $(\xi(\alpha), \eta(\alpha))$.
Since the contact force $\vec{f}$ is perpendicular to the profile function it can be described by

$$\vec{f} = f\big(\sin(\alpha)\vec{e}_x - \cos(\alpha)\vec{e}_y\big) \tag{6}$$

We have the bending moment about the z-axis:

$$m_{bz}(s) = \begin{cases} f\big((y(s) - \eta(\alpha))\sin(\alpha) + (x(s) - \xi(\alpha))\cos(\alpha)\big) & s \in [0, s_1) \\ 0 & s \in (s_1, 1] \end{cases} \tag{7}$$

with the condition for the setting moment m_0

$$m_{bz}(s \to 0) = -m_0 \tag{8}$$

Using (7) and introducing a differential equation for the curvature, the ODE system (5) can be rewritten as

$$\left.\begin{aligned} &(a) \quad x'(s) = \cos(\varphi(s)) \\ &(b) \quad y'(s) = \sin(\varphi(s)) \\ &(c) \quad \varphi'(s) = \kappa(s) \\ &(d) \quad \kappa'(s) = f\cos(\varphi(s) - \alpha) \end{aligned}\right\} \tag{9}$$

A distinction between tip and tangential contact of the rod with the object (phase A and phase B, respectively) is made (see Fig. 7).

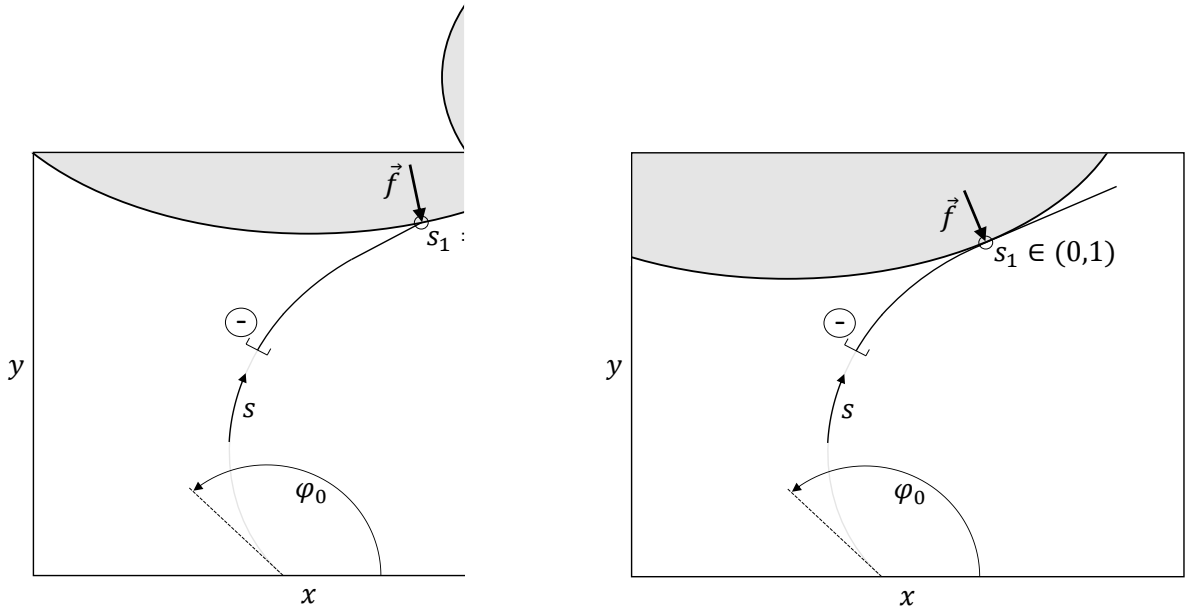

Figure 7. Contact scenarios: (a) Phase A (contact at the tip), (b) Phase B (tangential contact)

For both phases the boundary conditions are determined.

- **Phase A: Contact at the tip**

  Contact at the tip of the rod ($s_1 = 1$) with unknown $\varphi(1) > \alpha$:
  The ODE-system (13) is valid for $s \in [0, 1]$. The describing set of boundary conditions is given by

$$\begin{array}{llll} (a) & x(0) = x_0 & (e) & x(1) = \xi(\alpha) \\ (b) & y(0) = 0 & (f) & y(1) = \eta(\alpha) \\ (c) & \varphi(0) = \varphi_0 & & \\ (d) & \kappa(0) = c_t(\varphi(0) - \psi) & (g) & \kappa(1) = 0 \end{array} \tag{10}$$

- **Phase B: Tangential Contact**

  Contact at an unknown point $s_1 \in [0, 1)$ with $\varphi(s_1) = \alpha$:
  The ODE-system (13) is valid for $s \in [0, s_1)$. We have the boundary conditions

$$\begin{array}{llll} (a) & x(0) = x_0 & (e) & x(s_1) = \xi(\alpha) \\ (b) & y(0) = 0 & (f) & y(s_1) = \eta(\alpha) \\ (c) & \varphi(0) = \varphi_0 & (g) & \varphi(s_1) = \alpha \\ (d) & \kappa(0) = c_t(\varphi(0) - \psi) & (h) & \kappa(s_1) = 0 \end{array} \tag{11}$$

The boundary-value problems (13)&(10) and (13)&(11) can be solved using shooting methods to determine the unknown parameters f, α and s_1 (note that $s_1 = 1$ in presence of phase A). Therefore, an algorithm is created that is used for simulating the rotational sweep along a strictly convex object contour and generating the unknown observables (support reactions f_{Ax}, f_{Ay} and the setting moment m_0, that is required to set the angle φ_0).
In a next step, these observables are used for the reconstruction of the scanned profile by solving an initial-value problem, which is given by (13) and the following initial conditions at the base point:

$$x(0) = x_0, \quad y(0) = 0, \quad \varphi(0) = \varphi_0, \quad \kappa(0) = -m_0 \tag{12}$$

In this case, the parameters f and α in (13)(d) are not known, but can be specified as a function of the known support reactions:

$$f = \sqrt{f_{Ax}^2 + f_{Ax}^2} \quad \text{and} \quad \alpha = -\arctan\left(\frac{f_{Ax}}{f_{Ay}}\right) \tag{13}$$

Since we now have **all** parameters of (13)(d) the ODE can be integrated numerically. For determining the contact position s_1, we use the condition $\kappa(s_1) = m_{bz}(s_1) = 0$. Then, the contact point $(x(s_1), y(s_1))$ can be determined integrating (13)(a) and (b).

To improve the efficiency of the algorithm it is useful to have a condition for the distinction between phase A and phase B by means of the observables. Therefore, we present a criterion for the presence of phase B:

$$\boxed{m_0^2 - 2f_{Ay}\sin(\varphi_0) - 2f_{Ax}\cos(\varphi_0) = 0} \tag{14}$$

A condition for tangential contact has already been derived in previous publications for the **translationally scanning process** [24], see Fig. 5:

$$m_{Az} - 2f_{Ay} = 0 \tag{15}$$

Setting the control angle $\varphi_0 = \pi/2$ it becomes clear that (14) corresponds to (15).

5. SIMULATIONS

Here, we simulate a single rotational sweep along the following contour function:

$$g : x \mapsto g(x) = p\,x^2 + q$$

The support position is $x_0 = y_0 = 0$ and the parameter q is varied to investigate the influence of the object distance on the scanning process. The deformation states are shown in Fig. 8, where tip contacts (phase A) are blue colored and tangential contacts are red colored. The transitions between those phases are shown in black (the black state still belongs to the prior phase). The scanned area is limited by the profile parameters α_{Start} and α_{Ende}. Whereas α_{Start} results from the first contact between the undeflected rod and the object, α_{Ende} is defined by the last equilibrium state of the vibrissa, which is computed before the algorithm aborts.

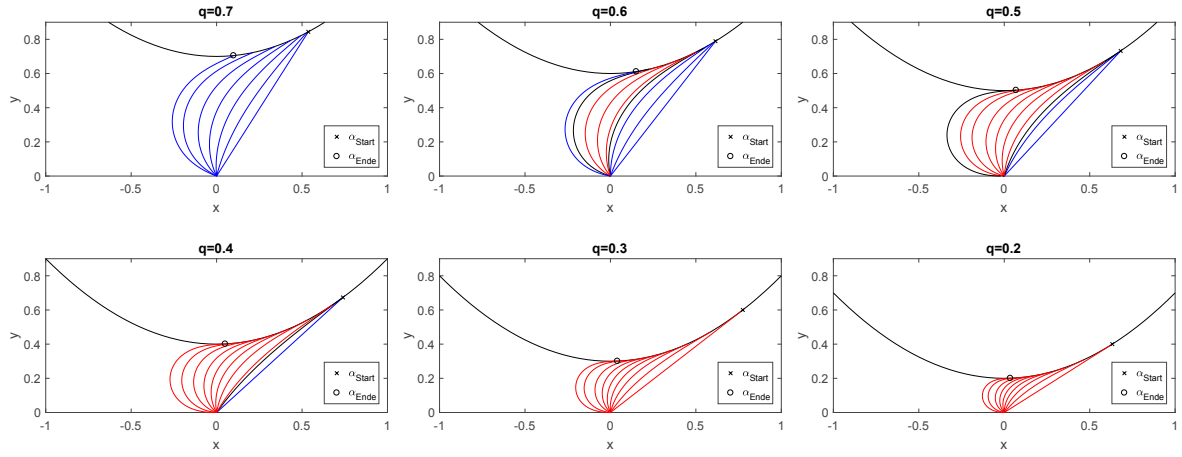

Figure 8. Scanning process with different object distances q

It can be observed that the size of the scanning range varies by changing the object distance q. In addition, it is clear that, with a large object distance, only tip contacts occur, whereas tangential contacts increasingly occur with decreasing object distance. Figure 9(a)-(c) shows the observables m_0, f_{Ax} and f_{Ay} plotted against the setting angle φ_0 (note that there is a varying notation for the setting angle φ_0 in Fig. 9: $\varphi_0 \hat{=} \psi$).

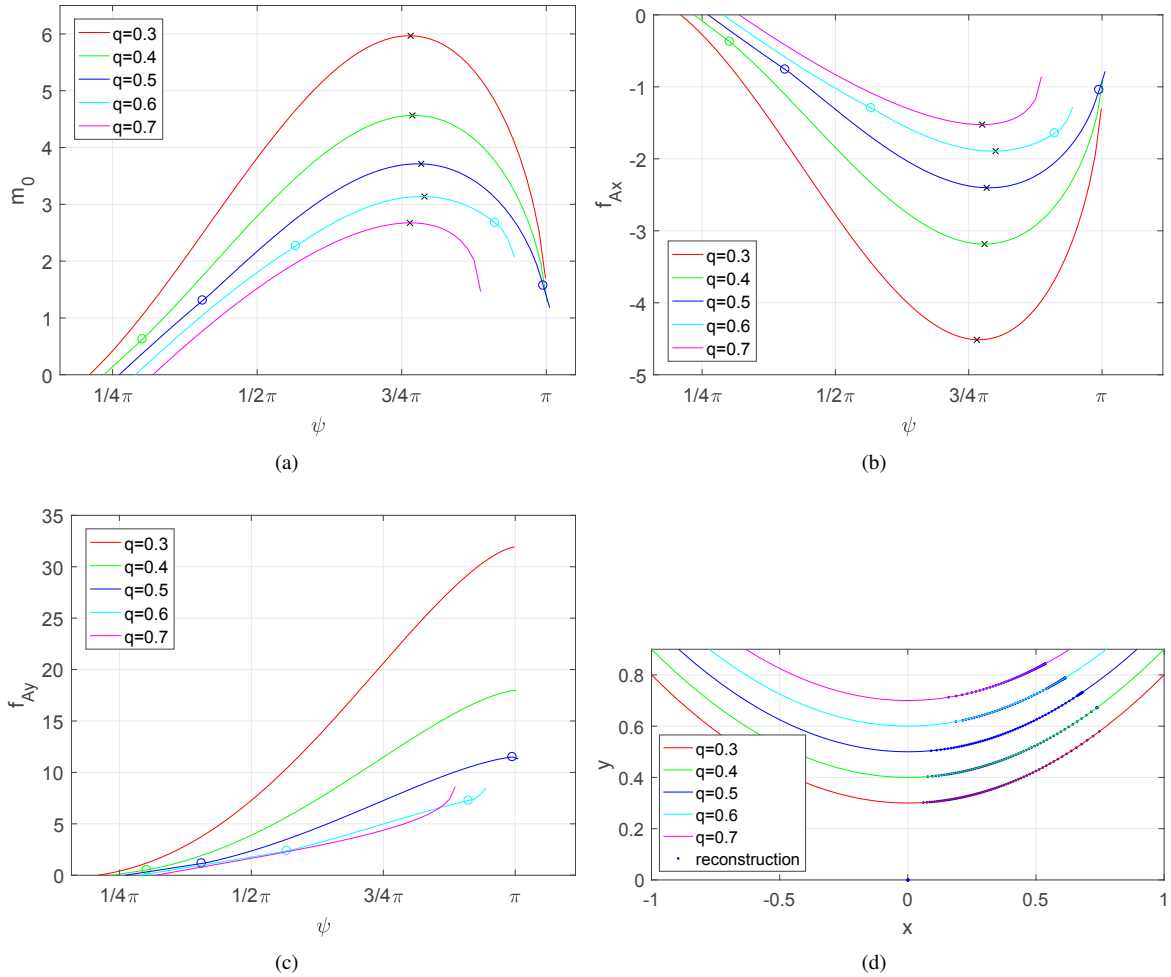

Figure 9. Scanning process with different parameters q

The extreme values are marked with an “x”. The phase transitions (see Fig. 8) are marked with an “o”.

(a) The setting moment m_0 begins to rise at the first contact between the rod and the profile. It reaches a maximum and then drops sharply until the algorithm terminates. The closer the object the higher is the maximum value of the required positioning torque.

(b) The magnitude of the bearing force f_{Ax} increases until reaching a maximum and then decreases until the algorithm terminates. As the object distance decreases, the amount of the bearing force f_{Ax} increases.

(c) The bearing force f_{Ay} increases strictly monotonously until the termination of the algorithm. The lower the object distance q, the steeper the gradient is.

(d) The object contours are outlined and overlaid with a sequence of reconstructed contact points for each scan. These sequences of reconstructed points where determined using condition (14) for the distinction of phase A and B, what serves as a validation for (14).

As Fig. 9(a)-(c) shows, it is possible to control the signal strength by varying the object distance q. Thus, the signal strength could be adapted for the measuring range of any sensor. Since we focus on a vibrissa rotation in mathematical positive sense, the scanning area is limited to the right side of the object (positive x-area).
To enlarge the reconstructable area, we extend the scanning process with a view on the biological paradigm. Because animals sweep their vibrissae back and forth along objects, from now on, we consider two rotational movements of the vibrissa – one in a mathematical positive sense and then another one in opposite direction.
Fig. 10(a) and (b) shows the extended scanning procedure using two different exemplary contour functions:

- **Example 1**: a parabola as used in Fig. 9: $g_1 : x \mapsto g_1(x) = 0.5x^2 + 0.3$

- **Example 2**: an asymmetric profile using a sectionally defined function:

$$g_3 : x \mapsto g_3(x) = \begin{cases} 0.5x^2 + 0.5 & (-1 \leq x < 0) \\ x^4 + 0.5 & (0 \leq x \leq 1) \end{cases}$$

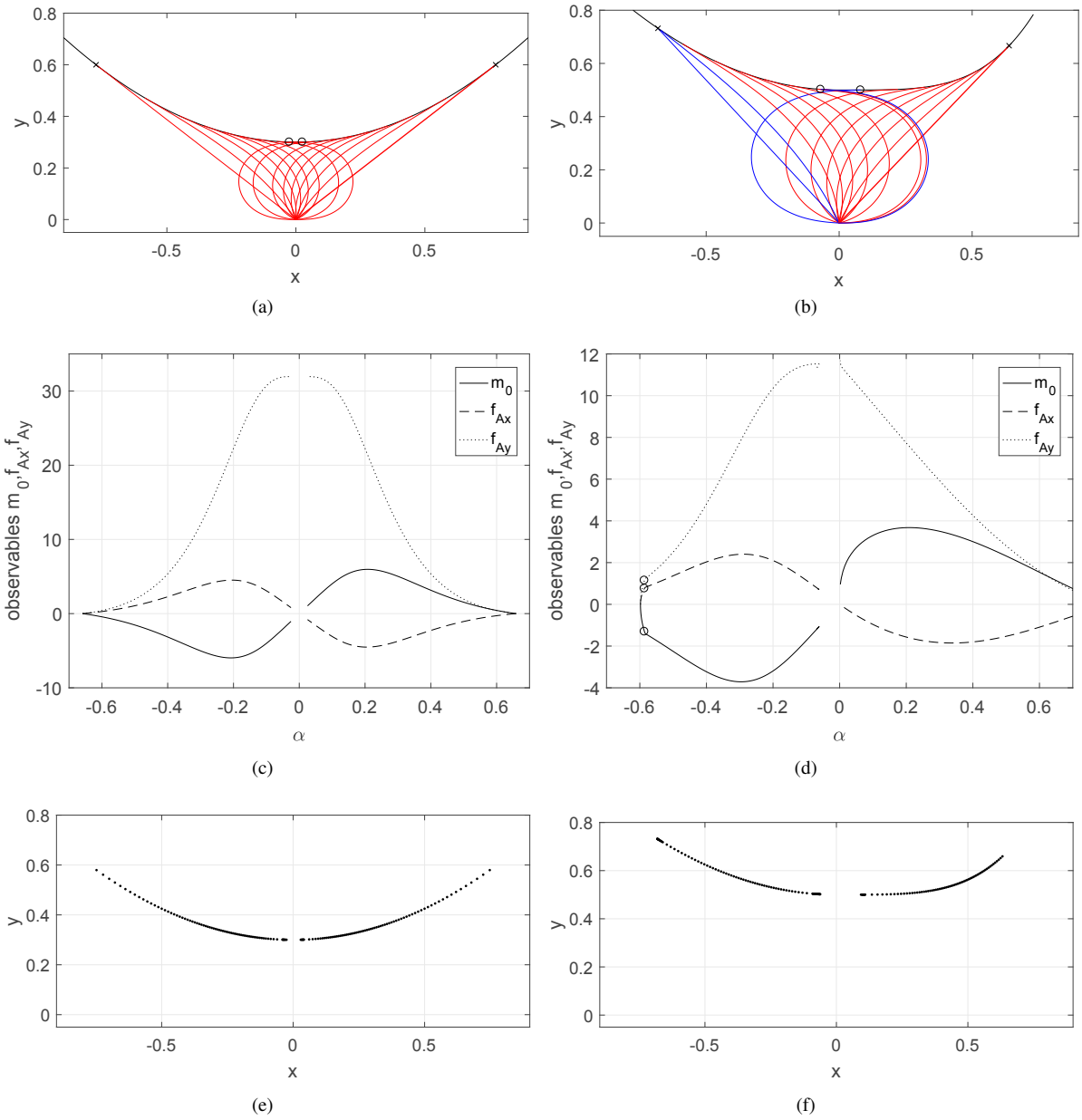

Figure 10. Scanning process for various object contour functions

The curves for the observables m_0, f_{Ax} and f_{Ay} are illustrated in Figs. 10(c) and (d). To give some information about the scanning range in addition, it is suitable to plot the observables against the slope angle α instead of the setting angle φ_0. Furthermore, Figs. 10(e) and (f) shows the reconstructed contact points using only the observables and informations about the support position.

- **Example 1**: Figure 10(a) shows that the size of the scanning range is significantly greater than in Fig. 8. Since the parabola is placed symmetrically relative to the support the scanning area (shown in Fig. 8) is mirrored at the y-axis by sweeping the vibrissa in opposite direction. This symmetry is also apparent looking at the observables in Fig. 10(c). The observables for $\alpha > 0$ result from the scanning movement in mathematical

positive sense, those for $\alpha < 0$ from the rotation in opposite direction. It can be observed, that the curves for the setting moment m_0 and the support reaction f_{Ax} are point symmetric. The curve for f_{Ay} is axial symmetric because the reaction force must be positive for both directions of rotation.

- **Example 2**: To show the general functionality of the algorithm we use another object shape, that is given by a sectionally defined contour function (asymmetric object). The asymmetry reappears in the curves for the observables (see Fig. 10(f)). In particular, the curves of f_{Ay} for the positive sweep and the negative sweep are qualitatively different.

We have seen that the reconstruction of the object works well for symmetric or asymmetric shapes. Nevertheless, the reconstructed ranges in both cases are severed by a small gap in the area of $\alpha = 0$. This gap results from the abort of the algorithm for both, the positive and the negative scanning rotation. In Figs. 10(a) and (b), the last contact point for each scan is marked with an "o". The according deformation state of the vibrissa is the last equilibrium that can be determined by the algorithm. It can be imagined that in reality after reaching a critical angle φ_0 the vibrissa would snap off of an object. The abort of the algorithm used for the simulations could point out that after reaching the last equilibrium state a further increase of the setting angle φ_0 would lead to the snapp off.

6. SUMMARY AND OUTLOOK

In this paper, we set up a biologically inspired mechanical model for tactile shape recognition. Therefore, the translationally scanning procedure, that is used in many preceded publications, was adapted for a rotational movement of the vibrissa, which is closer to the animals behavior during active whisking. The vibrissa was modeled as a cylindrically shaped Euler-Bernoulli bending rod, which is pivoted by a bearing. A single quasi-static sweep of the rod along a strictly convex contour function was analyzed using nonlinear Euler-Bernoulli theory. The investigation resulted in a set of ordinary differential equations, describing the deformation state of the vibrissa. After that, a distinction between tip and tangential contact of the vibrissa with the object (phase A and phase B, respectively) was made, and for both phases the boundary conditions were determined. The arose equations together with the boundary conditions form a general boundary-value problem with some unknown parameters. We presented an algorithm to determine these unknown parameters (e.g. the contact force) using shooting methods and to generate the support reactions as well as the setting moment during the rotational sweep of the vibrissa along a strictly convex profile. In a next step, the support reactions together with the boundary conditions at the support were used for the reconstruction of the object shape by solving an initial-value problem. We presented a condition for the distinction between phase A and phase B by means of the observables in order to improve the efficiency of the algorithm. This condition is a more general formulation compared with a similar criterion presented in [24] for translationally scanning.
First of all, the simulation algorithm was used for scanning a parabola by a single sweep. In particular, it was shown that the occurring observables could be manipulated, changing the object distance. The closer an object, the higher the extreme values of the observables. Thus, it is possible to control the signal strength with respect to the measuring range of any sensor. Furthermore, the investigation showed, that the scanning range of the profile was limited to the right side of the parabola. For that reason, in a next step, the scanning procedure was extended by rotating the vibrissa in opposite direction. In doing so, the reconstructable area could be enlarged. Two example simulations using different contour functions showed that the reconstructed areas in both cases were severed by a small gap, which results from the abort of the algorithm in both scanning directions. This observation might indicate a snap off of the vibrissa from the object, that would actually occur in reality.

Further studies should be conduced to investigate this snap off behavior more closely and to formulate a termination condition for the algorithm. Therefore, it is conceivable to simplify the object by a constant profile contour (note that such a profile is no longer strictly convex) and simulating the rotational sweep with different object distances. Thus, we could acquire a better understanding about which parameters influence the critical snap off angle $\varphi_{0,snap}$. This might enable us to reduce the size of the gaps in the scanning range (see Figs. 10(e) and (f)).

7. REFERENCES

[1] Behn, C., J. Steigenberger, A. Sauter and C. Will (2016): Pre-curved Beams as Technical Tactile Sensors for Object Shape Recognition; *The Fifth International Conference on Intelligent Systems and Applications (includes InManEnt 2016)*, pp. 7-12.

[2] Birdwell, J.A., J.H. Solomon, M. Thajchayapong, M.A. Taylor, M. Cheely, R.B. Towal, J. Conrad and M.J.Z. Hartmann (2007): Biomechanical Models for Radial Distance Determination by the Rat Vibrissal System; *Journal of Neurophysiology* 98(4), pp. 2439-2455.

[3] Carl, K. (2009): Technische Biologie des Tasthaar-Sinnessystems als Gestaltungsgrundlage für taktile stiftführende Mechanosensoren. PhD thesis, Ilmenau: Technische Universität Ilmenau, Germany.

[4] Clements, T.N. and C.D. Rahn (2006): Three-dimensional contact imaging with an actuated whisker; *IEEE Transactions on Robotics* 22(4), pp. 844-848.

[5] Dörfl, J. (1982): The musculature of the mystacial vibrissae of the white mouse; *Journal of anatomy* 135(1), pp. 147-154.

[6] Ebara, S., K. Kumamoto, T. Matsuura, J.E. Mazurkiewicz and F.L. Rice (2002): Similarities and differences in the innervation of mystacial vibrissal follicle-sinus complexes in the rat and cat: A confocal microscopic study; *The Journal of Comparative Neurology* 449(2), pp. 103-119.

[7] Fundin, B.T., K. Pfaller and F.L. Rice (1997): Different distributions of the sensory and autonomic innervation among the microvasculature of the rat mystacial pad; *The Journal of Comparative Neurology* 389(4), pp. 545-568.

[8] Hires, S.A., L. Pammer, K. Svoboda and D. Golomb (2013): Tapered whiskers are required for active tactile sensation; *eLife* 2.

[9] Hirose, S., S. Inoue and K. Yoneda (1989): The whisker sensor and the transmission of multiple sensor signals; *Advanced Robotics* 4(2), pp. 105-117.

[10] Jung, D. and A. Zelinsky (1996): Whisker Based Mobile Robot Navigation; in *Proceedings of IEEE/RSJ International Conference on Intelligent Robots and Systems. IROS '96*, pp. 497-504.

[11] Kim, D. and R. Möller (2007): Biomimetic whiskers for shape recognition; *Robotics and Autonomous Systems* 55(3), pp. 229-243.

[12] Merker, L.: Objektabtastung und -konturerkennung durch rotatorisch gelagerte, taktile Sensoren mittels nichtlinearer Balkentheorie, Master thesis, Ilmenau: Technische Universität Ilmenau, Germany.

[13] Mitchinson, B., R.A. Grant, K. Arkley, V. Rankov, I. Perkon and T.J. Prescott (2011): Active vibrissal sensing in rodents and marsupials; *Philosophical Transactions of the Royal Society B: Biological Sciences* 366(1581), pp. 3037-3048.

[14] Pammer, L., D.H. O'Connor, S.A. Hires, N.G. Clack, D. Huber, E.W. Myers and K. Svoboda (2013): The mechanical variables underlying object localization along the axis of the whisker; *The Journal of Neuroscience : the official journal of the Society for Neuroscience* 33(16), pp. 6726-6741.

[15] Quist, B.W., R.A. Faruqi und M.J.Z. Hartmann (2011): Variation in Young's modulus along the length of a rat vibrissa; *Journal of Biomechanics* 44(16), pp. 2775-2781.

[16] Quist, B.W. and M.J.Z. Hartmann (2012): Mechanical signals at the base of a rat vibrissa: the effect of intrinsic vibrissa curvature and implications for tactile exploration; *Journal of Neurophysiology* 107(9), pp. 2298-2312.

[17] Schierloh, A. (2003): Neuronale Netzwerke und deren Plastizität im Barrel-Kortex der Ratte. PhD thesis, Technical University of Munich, Germany.

[18] Scholz, G.R. and C.D. Rahn (2004): Profile Sensing With an Actuated Whisker; *IEEE Transactions on Robotics and Automation* 20(1), pp. 124-127.

[19] Solomon, J.H. and M.J.Z. Hartmann (2008): Artificial Whiskers Suitable for Array Implementation: Accounting for Lateral Slip and Surface Friction; *IEEE Transactions on Robotics* 24(5), pp. 1157-1167.

[20] Steigenberger, J. (2013): A continuum model of passive vibrissae. Preprint No. M13/03, Insitute of Mathematics, Technische Universität Ilmenau, Germany.

[21] Steigenberger, J., C. Behn and C. Will (2015): Mathematical model of vibrissae for surface texture detection. Preprint No. M15/03, Insitute of Mathematics, Technische Universität Ilmenau, Germany.

[22] Will, C., J. Steigenberger and C. Behn (2014): Object Contour Reconstruction using Bio-inspired Sensors; in *Proceedings of the 11th International Conference on Informatics in Control, Automation and Robotics*, pp. 459-467.

[23] Will, C., J. Steigenberger and C. Behn (2014): Quasi-static object scanning using technical vibrissae; in *Shaping the future by engineering: 58th IWK, Ilmenau Scientific Colloquium, Technische Universität Ilmenau, Germany*.

[24] Will, C., J. Steigenberger and C. Behn (2015): Obstacle scanning by technical vibrissae with compliant support. Preprint No. M13/03, Insitute of Mathematics, Technische Universität Ilmenau, Germany.

[25] http://www.laborjournal.de/rubric/archiv/stichwort/w_16_04.lasso, 19.07.2017, 8:20 Uhr